Monatsh Chem (2013) 144:761–772
DOI 10.1007/s00706-013-0961-3

ORIGINAL PAPER

Speciation of tin(II) in aqueous solution: thermodynamic and spectroscopic study of simple and mixed hydroxocarboxylate complexes

Rosalia Maria Cigala · Francesco Crea · Concetta De Stefano · Demetrio Milea · Silvio Sammartano · Michelangelo Scopelliti

Received: 23 October 2012 / Accepted: 5 March 2013 / Published online: 27 March 2013

Abstract This contribution reports the results of potentiometric and Mössbauer investigations on the formation, stability, and structure of binary and ternary mono- and binuclear complexes of Sn^{2+} with three hydroxocarboxylic ligands (namely L = tartrate, malate, and citrate) and chloride at $T = 298.15$ K in different ionic media and ionic strengths (0.15 and 1.00 mol dm^{-3} in $NaCl_{(aq)}$ and 1.00 mol dm^{-3} in $NaNO_{3(aq)}$). The stability constants of various simple $Sn_iH_jL_k^{(2i+j-kz)}$ and mixed $Sn_iH_jL_kCl_l^{(2i+j-kz-l)}$ species obtained in the different experimental conditions are reported, and various speciation diagrams of the simple and mixed systems are shown in different conditions. The sequestering ability of the three ligands toward Sn^{2+} was assessed by means of the calculation of the $pL_{0.5}$ parameter at different ionic strengths and in the different ionic media. The effect of the chloride anion on the stability of various species and on the sequestering ability of the investigated ligands toward Sn^{2+} was also evaluated. The structural results obtained by Mössbauer spectroscopy supported the speciation schemes obtained by the potentiometric investigations and indicated the possible trigonal bipyramidal arrangement of various Sn^{2+}/ligand species. Measurements at different temperatures were also performed in the case of citrate, in order to estimate the temperature dependence of the stability of these species. A modified version of the computer program STACO is briefly presented here for the first time and allows the simultaneous determination of the stability constants and the enthalpy changes of various species from potentiometric titrations at different temperatures.

Keywords Computer programs · Coordination chemistry · Metal complexes · Mössbauer spectroscopy · Sequestration · Stability constants

Introduction

Inorganic tin is rarely rated among the most common inorganic pollutants, though its presence in the environment is strictly linked to human activities. As a consequence, while the chemistry of organotin compounds has been extensively studied because of their high toxicity toward several living organisms, few works have been carried out on the inorganic forms of tin, whose speciation and chemical behavior are of great importance in understanding the activity of both inorganic and organic tin compounds. In fact, the alkylation of inorganic tin frequently occurs in the environment, as a consequence of biotic and abiotic activities, and it is influenced by its speciation. Moreover, tin is also present in the nuclear waste from fission as ^{126}Sn, with a half-life close to 10^5 years, so that a better knowledge of the chemistry of inorganic tin is essential to understand and model the speciation of these environmentally important systems [1–6]. Nevertheless, there are few reported speciation studies on inorganic tin in aqueous solution, and the available thermodynamic data allow only rough estimations [7]. In

For previous contributions in this series, see Refs. [1–3].

R. M. Cigala · F. Crea · C. De Stefano (✉) · D. Milea · S. Sammartano
Dipartimento di Scienze Chimiche, Università di Messina, Viale F. Stagno d'Alcontres, 31, 98166 Messina, Vill. S. Agata, Italy
e-mail: cdestefano@unime.it

M. Scopelliti
Dipartimento di Fisica e Chimica, Università di Palermo, Viale delle Scienze, 90128 Palermo, Italy

particular, the solution behavior of tin(II) is still approximately defined. Therefore we have recently undertaken a study of tin(II) speciation in aqueous solution [1–3]. As a first step, we defined both the acid–base properties and the inorganic speciation of tin(II) with the most important natural inorganic ligands, such as OH^-, Cl^-, F^-, CO_3^{2-}, SO_4^{2-} [1], and phosphates [2]. We then extended this study to tin(II) speciation in the presence of an organic ligand of biological and environmental relevance, namely phytate, and the formation of binary and ternary complexes with Cl^- and F^- [3].

As an extension of this study, this contribution reports some results of potentiometric and Mössbauer investigations at $T = 298.15$ K in different ionic media and ionic strengths (0.15 and 1.00 mol dm^{-3} in $NaCl_{(aq)}$ and 1.00 mol dm^{-3} in $NaNO_{3(aq)}$), on the formation, stability, and structure of Sn^{2+} complexes with three hydroxocarboxylic ligands, namely tartrate (Tar), malate (Mala), and citrate (Cit). The importance of the three investigated ligands is very well known, both from a biological and environmental point of view. New functions and applications are being continuously discovered, and this explains the huge number of studies on these ligands. A comprehensive description of these aspects is beyond the scope of this manuscript. Here we therefore just remark that they are involved in a variety of physiological functions and play key roles in several biochemical processes [8]. For example, both malate and citrate are involved in one of the most important biochemical processes, the Krebs cycle, also known as the tricarboxylic acid cycle or as the citric acid cycle, as a proof of the importance of this ligand [8]. Moreover, their very low cost, low toxicity, and great binding ability toward several metal and organometal cations (as well as other ligands) favor their use in the industrial and environmental fields.

These investigations are very important in multicomponent solutions such as natural waters, seawater, sewage, and biological fluids, where the simultaneous presence of several components in wide concentration ranges leads to the formation both of simple and ternary and/or quaternary MHLX species (M = generic metal ion, L = generic organic ligand, X = inorganic ligand; charge omitted for simplicity). In particular, the investigations on the formation of mixed species with Cl^- are fundamental, this anion being a major inorganic component of natural and biological fluids. Of course, the formation of other mixed species with other anions, such as SO_4^{2-}, HCO_3^-, and PO_4^{3-}, can be taken into account. These components are present in lower amounts in natural systems and show generally a higher binding ability towards the metal ions with respect to Cl^- [2, 9].

The potentiometric investigations carried out at $I = 1.00$ mol dm^{-3} in two different ionic media (i.e., $NaCl_{(aq)}$ and $NaNO_{3(aq)}$) allowed us also to observe a significant "medium" effect (the anion of the supporting electrolyte) on the stability of the various species, because it is well known [1] that Sn^{2+} forms three stable complexes with Cl^- ($SnCl_l^{(2-l)}$; $l = 1$–3) at also low concentrations, whereas nitrate can be considered as a weakly interacting medium toward this cation. As a consequence, the speciation of the different tin(II)/ligand systems in chloride media was evaluated by means of two different approaches. The first takes into account the conditional stability constants in $NaCl_{(aq)}$ without considering the influence of the ions of the supporting electrolytes on the formation of the species, whereas the second takes into account the formation of mixed Sn^{2+}/L/Cl^- species formed at high chloride concentrations. These two approaches are equivalent to explain the speciation of the systems.

The sequestering ability of the three investigated ligands toward Sn^{2+} was then evaluated in different conditions (pH, ionic strength, ionic medium) by means of the $pL_{0.5}$, a semi-empirical parameter already proposed in many papers for an objective quantification of this ability (see, e.g., Refs. [10–17]). Numerically, it represents the ligand concentration necessary to sequester 50 % of the metal ion and can be used for a fast comparison and measure of the sequestering abilities of different ligands in different conditions.

Mössbauer investigations were finally performed on various Sn^{2+}/ligand systems with the double aim of confirming the speciation models proposed by the potentiometric investigations and providing structural information about the coordination behavior of Sn^{2+} in the presence of the investigated ligands.

Finally, for the Sn^{2+}/citrate system, measurements at different temperatures were also performed, in order to estimate the temperature dependence of the stability of these species. In this context, a modified version of the computer program STACO [18], TSTACO, is briefly presented here for the first time and allows the simultaneous determination of the stability constants and the enthalpy changes of various species from potentiometric titrations at different temperatures.

Results and discussion

Inorganic speciation of Sn^{2+} and ligand protonation

We recently studied the interaction of Sn^{2+} with the most important inorganic ligands present in natural fluids, including OH^- and Cl^- [1]. Both the hydrolysis and the formation constants of chloride complexes were determined at $T = 298.15$ K in a wide range of ionic strengths and in different ionic media, and the values used in this paper were taken from that reference.

Concerning the acid–base properties of the three investigated ligands, the protonation constants calculated in the same medium and ionic strength conditions of this work were taken from Ref. [19]. The hydrolysis constants of Sn^{2+} and the stability constants of its chloride complexes as well as the ligand protonation constants are reported in Table 1.

Conditional formation constants and distribution of Sn^{2+}/tartrate species

The potentiometric data collected to analyze the Sn^{2+}/ligand systems in the different experimental conditions were processed with the STACO and BSTAC computer programs (see "Experimental"). Table 2 reports the formation constants for the Sn^{2+}/Tar system in different experimental conditions, i.e., $I = 0.15$ mol dm^{-3} in $NaCl_{(aq)}$ and $I = 1.00$ mol dm^{-3} in $NaNO_{3(aq)}$.

In these conditions, the proposed speciation scheme is SnTar, SnTarOH, $SnTar(OH)_2$, $SnTar_2OH$, $Sn_2Tar_2(OH)_2$, and $Sn_2Tar_2(OH)_3$. Without any initial structural information, this speciation scheme was selected as the best model, after several trials considering other different species. In fact, several elaborations were performed in order to select the best model, and an accurate statistical analysis of the results obtained from the different possible models was necessary (see, e.g., Refs. [20–22]). The ultimate criteria used to select the chemical model were (a) the value of the variance ratio; (b) the simplicity of the model (other minor species can be added to the chosen ones but the models become unrealistically complicated); (c) the likelihood of the proposed species, in particular in relation to the formation percentages and the pH range where they form; (d) the consistency of various models in the different conditions. By analyzing values in Table 2, we can also make some further comments: (i) independently of the ionic strength and ionic medium, the same speciation model was obtained; (ii) data at $I = 1.00$ mol dm^{-3} in $NaNO_{3(aq)}$ are significantly lower than the corresponding values at $I = 0.15$ mol dm^{-3} in $NaCl_{(aq)}$. The latter aspect can be explained by taking into account both the different ionic strength and the different interacting ability of the two anions of the supporting electrolytes.

In Fig. 1 we report the distribution of the Sn^{2+}/Tar species.

Even if low component concentrations were used, high formation percentages of the species were observed. In fact, the SnTar and the $SnTar(OH)_2$ species both reach ~70 %. The formation of the polynuclear $Sn_2Tar_2(OH)_3$ species is also very important; this occurs in the whole investigated pH range, achieving ~55 % at pH 4.6. At pH greater than 6.0–6.2, the formation of the sparingly soluble $Sn(OH)_{2(s)}$ species was sometimes observed in some (not all) experimental conditions, especially in the experiments performed at lower c_{Sn}/c_L ratios and higher metal concentrations. In the light of the above considerations, we propose to consider the speciation model and the stability constants obtained as "reliable" up to pH ~6.0.

Conditional formation constants and distribution of Sn^{2+}/malate species

The significant differences observed in the Sn^{2+}/tartrate system between the two different conditions led us to

Table 1 Hydrolysis constants of Sn^{2+}, stability constants of Sn^{2+}/Cl^- complexes, and protonation constants of tartrate, malate, and citrate used in this work at $T = 298.15$ K

Species	log β_{ijkl}^{a}		Species	log β_{ijkl}^{a}	
	$I = 0.15$ mol dm^{-3}	$I = 1.00$ mol dm^{-3}		$I = 0.15$ mol dm^{-3}	$I = 1.00$ mol dm^{-3}
Sn(OH)	−3.78[b]	−4.00[b]	HTar	3.894[c]	3.775[c]
$Sn(OH)_{2(aq)}$	−6.53	−6.81	H_2Tar	6.700	6.449
$Sn(OH)_3$	−16.97	−17.15			
$Sn_2(OH)_2$	−5.06	−5.32	HMala	4.63[c]	4.45[c]
$Sn_3(OH)_4$	−6.39	−6.80	H_2Mala	7.86	7.61
SnCl(OH)	−2.07	−2.61			
$Sn(OH)_{2(s)}$[d]	25.58	25.41	HCit	5.64[c]	5.22[c]
			H_2Cit	9.91	9.29
SnCl	0.76[b]	0.49[b]	H_3Cit	12.79	12.03
$SnCl_2$	1.50	1.09			
$SnCl_3$	1.46	1.05			

[a] log β_{ijkl} values refer to Eq. (2)

[b] Ref. [1]

[c] Ref. [19]

[d] Equilibrium: $Sn^{2+} + 2OH^- = Sn(OH)_{2(s)}$, log K_{s0}

Table 2 Experimental stability constants of $Sn_iH_jTar_k^{(2i+j-kz)}$ species at $T = 298.15$ K in different ionic media and ionic strengths

Species	log β_{ijkl}^{a}	
	NaCl $I = 0.15$ mol dm^{-3}	$NaNO_3$ $I = 1.00$ mol dm^{-3}
SnTar	6.26 ± 0.14	4.76 ± 0.01
SnTarOH	3.85 ± 0.10	1.20 ± 0.10
$SnTar(OH)_2$	−0.42 ± 0.11	−2.84 ± 0.03
$SnTar_2OH$	6.62 ± 0.11	4.18 ± 0.03
$Sn_2Tar_2(OH)_2$	11.35 ± 0.19	6.07 ± 0.02
$Sn_2Tar_2(OH)_3$	7.55 ± 0.15	2.76 ± 0.03

Data are reported as mean ± standard deviation

[a] log β_{ijkl} values refer to Eq. (2)

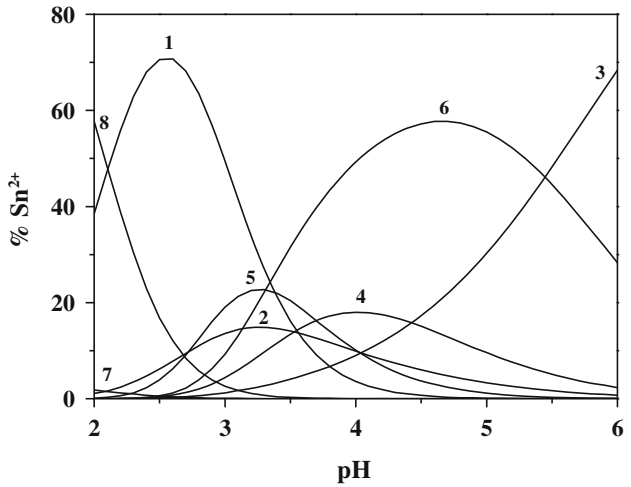

Fig. 1 Distribution diagram of Sn^{2+}/Tar species in $NaNO_{3(aq)}$ at $I = 1.00$ mol dm^{-3} and $T = 298.15$ K. Experimental conditions: $c_{Sn} = 1.1$ mmol dm^{-3}, $c_{Tar} = 4.4$ mmol dm^{-3}, $c_{Cl} = 3.2$ mmol dm^{-3}. Curves: *1* SnTar, *2* SnTarOH, *3* $SnTar(OH)_2$, *4* $SnTar_2OH$, *5* $Sn_2Tar_2(OH)_2$, *6* $Sn_2Tar_2(OH)_3$, *7* SnCl, *8* free Sn^{2+}

investigate this effect, in order to evaluate if these differences were mainly due to ionic strength changes or if the ionic medium effect was also important. As a consequence, in the case of the Sn^{2+}/Mala system, we performed further measurements at $I = 1.00$ mol dm^{-3} in $NaCl_{(aq)}$, in addition to the other ionic strength and medium conditions investigated in the case of tartrate (i.e., $I = 0.15$ mol dm^{-3} in $NaCl_{(aq)}$ and 1.00 mol dm^{-3} in $NaNO_{3(aq)}$). Concerning the Sn^{2+}/Mala system, in the experimental conditions adopted, the speciation scheme proposed consists of five species, namely SnHMala, SnMala, SnMalaOH, $SnMala_2$, and $Sn_2Mala_2(OH)_2$, whose stability constants are reported in the first part of Table 3.

The considerations discussed in relation to Sn^{2+}/tartrate about the reliability of the proposed model hold also in this case. Similar discussion about the stability of various species can also be done. Also in this system, the same speciation model was obtained in the three different conditions. As regards the effect of ionic strength, the results in Table 3 show that in the same ionic medium (i.e., $NaCl_{(aq)}$) except for the SnMala species, all other stability constant values are generally higher at $I = 1.00$ mol dm^{-3} than at $I = 0.15$ mol dm^{-3}. However, these differences are not as marked as in the case of the stability constants obtained at the same ionic strength (i.e., $I = 1.00$ mol dm^{-3}) but in different ionic media (values in $NaCl_{(aq)}$ are higher than those in $NaNO_{3(aq)}$). This is an indication of the greater influence on the stability of the ionic medium effect than the ionic strength. This is also evidenced by the analysis of Figs. 2 and 3.

Figure 2 reports the distribution diagram of the conditional Sn^{2+}/Mala system in $NaCl_{(aq)}$ at $I = 1.00$ mol dm^{-3}. As can be noted, the formation percentages of the complexes are rather high, and all exceed 25 %. However, from the analysis of this diagram, other important information can be obtained: (i) for pH values below pH ~4.6, we observe the presence of the simple $SnCl_l^{(2-l)}$ species, as well as the

Table 3 Experimental stability constants of $Sn_iH_jMala_k^{(2i+j-kz)}$ and $Sn_iH_jMala_kCl_l^{(2i+j-kz-l)}$ species at $T = 298.15$ K in different ionic media and ionic strengths

Species	log β_{ijkl}^{a}		
	NaCl		$NaNO_3$
	$I = 0.15$ mol dm^{-3}	$I = 1.00$ mol dm^{-3}	$I = 1.00$ mol dm^{-3}
SnHMala	8.66 ± 0.07	9.34 ± 0.03	7.48 ± 0.04
SnMala	6.02 ± 0.03	5.93 ± 0.02	5.06 ± 0.01
SnMalaOH	1.25 ± 0.10	1.54 ± 0.07	0.75 ± 0.05
$SnMala_2$	8.55 ± 0.04	9.04 ± 0.02	7.95 ± 0.02
$Sn_2Mala_2(OH)_2$	5.18 ± 0.06	6.56 ± 0.08	5.16 ± 0.03
SnHMalaCl		9.35 ± 0.03	
SnMalaCl		5.88 ± 0.02	
$SnMala_2Cl$		9.01 ± 0.03	
$Sn_2Mala_2Cl(OH)_2$		6.71 ± 0.01	

Data are reported as mean ± standard deviation

[a] log β_{ijkl} values refer to Eq. (2)

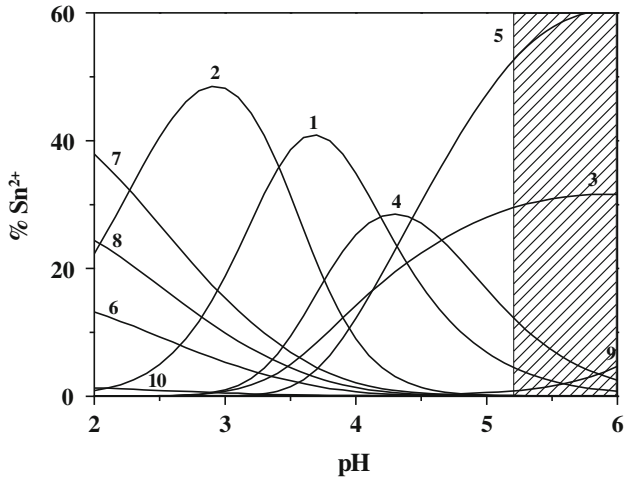

Fig. 2 Distribution diagram of Sn^{2+}/Mala species in $NaCl_{(aq)}$ at $I = 1.00$ mol dm^{-3} and at $T = 298.15$ K (conditional model). Experimental conditions: $c_{Sn} = 1.0$ mmol dm^{-3}, $c_{Mala} = 3.6$ mmol dm^{-3}, $c_{Cl} = 1.00$ mol dm^{-3}. Curves: *1* SnMala, *2* SnHMala, *3* SnMalaOH, *4* $SnMala_2$, *5* $Sn_2Mala_2(OH)_2$, *6* SnCl, *7* $SnCl_2$, *8* $SnCl_3$, *9* $Sn(OH)_{2(aq)}$, *10* free Sn^{2+}

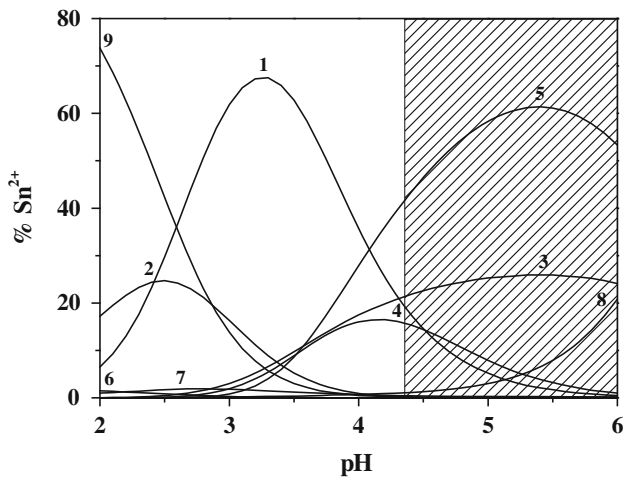

Fig. 3 Distribution diagram of Sn^{2+}/Mala species in $NaNO_{3(aq)}$ at $I = 1.00$ mol dm^{-3} and at $T = 298.15$ K. Experimental conditions: $c_{Sn} = 1.0$ mmol dm^{-3}, $c_{Mala} = 3.6$ mmol dm^{-3}, $c_{Cl} = 2.0$ mmol dm^{-3}. Curves: *1* SnMala, *2* SnHMala, *3* SnMalaOH, *4* $SnMala_2$, *5* $Sn_2Mala_2(OH)_2$, *6* SnCl, *7* SnOH, *8* $Sn(OH)_{2(aq)}$, *9* free Sn^{2+}

SnMala, SnHMala, and $SnMala_2$ species; (ii) for pH $\geq$3.6, there is the presence of the Sn^{2+} mixed hydrolytic species, and in particular we observe the $Sn_2Mala_2(OH)_2$ and SnMala(OH) species, which become the most important over pH $\sim$5; (iii) for higher pH values, the neutral hydrolytic species of Sn^{2+}, $Sn(OH)_{2(aq)}$, is formed. Above this pH (corresponding to the shaded zone in Fig. 2), as for the tartrate system, the formation of the sparingly soluble $Sn(OH)_{2(s)}$ species was sometimes observed. That is why we propose to consider the speciation model and the stability constants obtained in these conditions as "reliable" up to pH $\sim$5.2.

Table 4 Experimental stability constants of $Sn_iH_jCit_k^{(2i+j-kz)}$ and Sn_iH_j-$Cit_kCl_l^{(2i+j-kz-l)}$ species at $T = 298.15$ K in different ionic media and ionic strengths

Species	log β_{ijkl}^{a}		
	NaCl		$NaNO_3$
	$I = 0.15$ mol dm^{-3}	$I = 1.00$ mol dm^{-3}	$I = 1.00$ mol dm^{-3}
SnCit	8.389 ± 0.006		7.349 ± 0.009
SnCitOH	4.041 ± 0.007		2.995 ± 0.008
$SnCit(OH)_2$	−2.489 ± 0.006		−5.56 ± 0.06
$Sn_2H_2Cit_2$	27.26 ± 0.02		24.22 ± 0.04
Sn_2HCit_2	24.49 ± 0.01		21.02 ± 0.06
Sn_2Cit_2	20.822 ± 0.009		18.10 ± 0.04
Sn_2Cit_2OH	15.68 ± 0.01		13.64 ± 0.04
$Sn_2Cit_2(OH)_2$	10.81 ± 0.01		9.15 ± 0.04
SnCitCl		7.60 ± 0.06	
SnCitClOH		3.06 ± 0.05	
Sn_2HCit_2Cl		22.25 ± 0.06	

Data are reported as mean ± standard deviation

[a] log β_{ijkl} values refer to Eq. (2)

A quite similar speciation diagram is obtained in $NaNO_{3(aq)}$ at $I = 1.00$ mol dm^{-3} (Fig. 3), though some other important considerations should be made. Owing to the absence of the $SnCl_l^{(2-l)}$ species at low pH ($\sim$2) values, the presence of free Sn^{2+} reaches $\sim$75 %. At the same time, the peaks of formation of all species are shifted towards lower pH values in $NaNO_{3(aq)}$ than in $NaCl_{(aq)}$. Moreover, the $Sn(OH)_{2(aq)}$ species becomes significant at pH $\sim$4.4, about 0.8 log units lower than in $NaCl_{(aq)}$. In this condition the "reliability" of the model is then lowered at pH 4.4.

Conditional formation constants and distribution of Sn^{2+}/citrate species

Similarly to the Sn^{2+}/Mala system, the experimental data of citrate were processed using the procedures reported above. The speciation model that gave the best result is represented by the following species: SnCit, SnCitOH, $SnCit(OH)_2$, $Sn_2H_2Cit_2$, Sn_2HCit_2, Sn_2Cit_2, $Sn_2Cit_2(OH)$, and $Sn_2Cit_2(OH)_2$. As can be noted, this model is much more complicated than the previous Sn^{2+}/Mala system, and can be explained by taking into account the strong sequestering ability of citrate toward several metal ions and its tendency to form polynuclear and/or simple or ternary mixed ligand (chloride in our case) complexes. In fact, similar evidence was obtained in a previous investigation on the sequestration of dioxouranium(VI) by citrate in $NaCl_{(aq)}$ [15]. From a rough comparison between the Mala and Cit systems, it is also possible to observe that the formation constants of the Sn^{2+}/Cit complexes (Table 4)

are significantly higher than those of Mala, independently of the ionic strength and of the ionic medium.

All these aspects contribute to increase the investigable pH range of the Sn^{2+}/Cit system with respect, for example, to the Sn^{2+}/Mala, as a result of the stronger ability of citrate to hamper the formation of the hydrolytic $Sn(OH)_{2(s)}$ species.

Though the elaboration of data obtained for the Sn^{2+}/Cit system at two different ionic strengths and in two different ionic media (i.e., at $I = 0.15$ mol dm^{-3} in $NaCl_{(aq)}$ and $I = 1.00$ mol dm^{-3} in $NaNO_{3(aq)}$) gave the same results in terms of speciation schemes, the complexity of this system led us to perform further checks, in addition to the approach described for the Sn^{2+}/Mala system. After the determination of the stability constants of Sn^{2+}/Cit complexes at $I = 1.00$ mol dm^{-3} in $NaCl_{(aq)}$, all data at $I = 1.00$ mol dm^{-3} in $NaCl_{(aq)}$ and $NaNO_{3(aq)}$ were re-elaborated together (of course taking into account the formation of chloride complexes, see next paragraph) by the BSTAC and STACO programs. Though this procedure did not allow us to determine any conditional stability constant in $NaCl_{(aq)}$, it acted as a further proof of the validity of the speciation model. In fact, by the simultaneous elaboration of a great number of measurements for the same system in different conditions we have been able to obtain the same (within the experimental errors) values of the stability constants and the same speciation scheme previously determined from the elaboration of measurements in $NaNO_{3(aq)}$ only. Because of the aforementioned complexity of the system and the great number of measurements performed, this consistency of results allowed us to be more "confident" about the proposed model. The formation of the mixed Sn^{2+}/Cit/Cl^- species and their influence on citrate and tin(II) speciation will be detailed in the next section. Nevertheless, it is important to affirm here that, for the same considerations made in the case of malate, the proposed speciation scheme can be considered "reliable" up to pH ~6.5.

Formation constants of mixed Sn^{2+}/ligand/Cl^- species

In the past, our research group has been involved in studies of the formation of mixed species for many different metals with organic and inorganic ligands [22–25].

Results reported above for the malate and citrate systems led us to investigate the possible formation of the ternary $Sn_iH_jL_kCl_l^{(2i+j-kz-l)}$ (L = Mala or Cit) species. Moreover, we have already observed that this kind of mixed ligand/chloride (and/or fluoride) species is easily formed by Sn^{2+} [3]. The data analysis evidenced the formation of both mono- and binuclear ternary complex species, with different numbers of protons or hydroxo groups involved into the complex formation (see Tables 3 and 4 for Mala and Cit, respectively). Other ternary complexes were checked but discarded, because they were systematically rejected from the computer programs or because the presence of these species in the speciation scheme did not significantly improve the goodness of fit.

The study of the Sn^{2+}/ligand systems in $NaCl_{(aq)}$ can be approached in two ways: (1) by determining only the conditional stability constants in particular conditions of ionic strength and ionic medium; (2) by determining and taking into account the stability constants of both the "simple" Sn^{2+}/ligand complexes in a weakly interacting medium ($NaNO_{3(aq)}$) and the ternary mixed ligand (chloride in our case) species, which allow one to explain the differences of the stability constants between the two ionic media. This second option better works for speciation purposes, because it gives the possibility to model the speciation of Sn^{2+}/ligand systems in a wider range of experimental conditions.

The higher stability constants in $NaCl_{(aq)}$ than $NaNO_{3(aq)}$ can be explained by taking into account the stabilizing effect of Cl^- toward the formation of the mixed Sn^{2+}/Mala/Cl^- and Sn^{2+}/Cit/Cl^- complexes.

Figure 4 reports the distribution of the species for the Sn^{2+}/Mala/Cl^- system. We observe that the formation percentage of the SnHMalaCl species reaches about ~52 % at pH ~2.8, and that the other mixed complexes, namely SnMalaCl and $SnMala_2Cl$, reach ~40 and 30 %, respectively. The $Sn_2Mala_2Cl(OH)_2$ is formed at pH ~3.6 and reaches ~80 % at pH ~6, avoiding the formation of the $Sn(OH)_{2(aq)}$ in significant amounts (this species does not exceed 5 %). Taking into account this approach, the simple Sn^{2+}/Mala complexes are formed in small amount

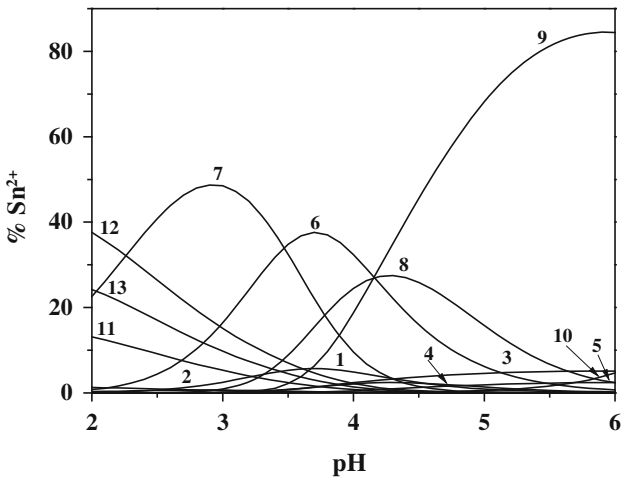

Fig. 4 Distribution diagram of Sn^{2+}/Mala and Sn^{2+}/Mala/Cl^- species at $T = 298.15$ K. Experimental conditions: $c_{Sn} = 0.5$ mmol dm^{-3}, $c_{Mala} = 3.6$ mmol dm^{-3}, $c_{Cl} = 1.00$ mol dm^{-3}. Curves: *1* SnMala, *2* SnHMala, *3* SnMalaOH, *4* $SnMala_2$, *5* $Sn_2Mala_2(OH)_2$, *6* SnMalaCl, *7* SnHMalaCl, *8* $SnMala_2Cl$, *9* $Sn_2Mala_2Cl(OH)_2$, *10* $Sn(OH)_{2(aq)}$, *11* SnCl, *12* $SnCl_2$, *13* $SnCl_3$

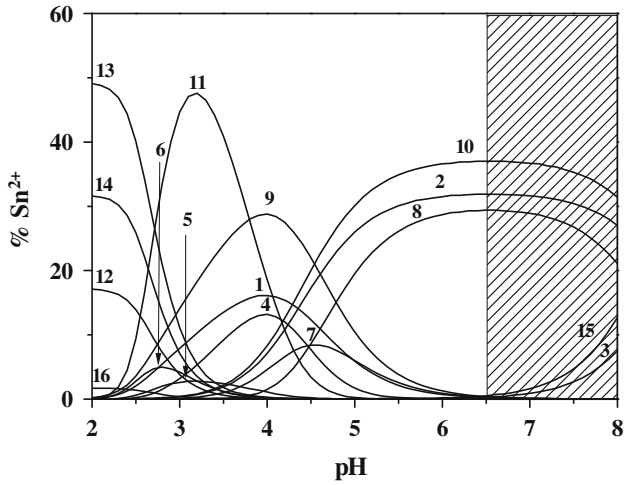

Fig. 5 Distribution diagram of Sn^{2+}/Cit and Sn^{2+}/Cit/Cl^- species at $I = 1.00$ mol dm^{-3} and at $T = 298.15$ K. Experimental conditions: $c_{Sn} = 1.0$ mmol dm^{-3}, $c_{Cit} = 3.7$ mmol dm^{-3}, $c_{Cl} = 1.00$ mol dm^{-3}. Curves: *1* SnCit, *2* SnCitOH, *3* $SnCitOH_2$, *4* Sn_2Cit_2, *5* Sn_2HCit_2, *6* $Sn_2H_2Cit_2$, *7* Sn_2Cit_2OH, *8* $Sn_2Cit_2(OH)_2$, *9* SnCitCl, *10* SnCitClOH, *11* Sn_2HCit_2Cl, *12* SnCl, *13* $SnCl_2$, *14* $SnCl_3$, *15* $Sn(OH)_{2(aq)}$, *16* free Sn^{2+}

($\leq \sim 10$ %). Similar behavior is shown by the already described Sn^{2+}/Cit system, whose speciation diagram is shown in Fig. 5.

All the mixed Sn^{2+}/Cit/Cl^- species reach high formation percentages, about 30–50 %. The "simple" Sn^{2+}/Cit species are formed, too, in significant amounts. For example, the SnCitOH and the $Sn_2Cit_2(OH)_2$ reach formation percentages higher than 20 %, whilst the other Sn^{2+}/Cit species reach $\sim$10–15 %. As already stated, in this case, the reliability of the speciation model can be considered up to pH $\sim$6.5. In fact, above this pH value the $Sn(OH)_{2(aq)}$ species would be formed in significant amounts, and would be in equilibrium with the corresponding solid species (see shaded zone in Fig. 5).

These results also demonstrate that the formation of the mixed species during calculations by computer programs is not a fictitious improvement in fittings arising from a simple minimization of experimental errors.

Mössbauer spectroscopy

Mössbauer spectroscopy has been applied to study equilibria in aqueous solution by means of quick-freezing technique. Quick-freezing solutions are commonly used in Mössbauer spectroscopy to characterize solution species. The rapid freezing of a solution (at equilibrium) creates a quasi-homogeneous lattice without the orientating effects of a crystal structure, thus permitting useful measurements. The resulting spectra can be studied as a sum of subspectra of observable species, each subspectrum weighted by the relative abundance in the starting solution.

Mössbauer data were analyzed assuming all absorbing profiles as Lorentzian in shape. For a given lattice, Γ (FWHM) was held constant. Contributions of species below 10 % were neglected; to compensate the lacking area, a "ghost peak", cumulative of all minor components and without Γ restraints, was used. Dinuclear species were treated as two independent absorbers with forced abundance ratio (1:1).

Once characterized at a specific pH value, the obtained parameters were used as a constraint for the same species at different pH. This technique was used iteratively on the suitably sampled speciation diagram, until self-consistency, thereby validating the diagram itself.

In the case of citrate, even if the system is well characterized in terms of relative abundance of observed species, it is not possible to assess structural information, because there is not an effective model such as for Sn^{4+}. Some tentative models were built in the early 1980s [26–28], but they lack rationalization and are not applicable to solutions in a straightforward way (besides, their applicability has yet to be proved). Table 5 reports the obtained values for tin(II) Mössbauer spectra analysis.

It must be remembered that the protonation of the organic moieties has no effect on Mössbauer absorption: only three groups of species (one mononuclear and two dinuclear) are reported. The only structural guess for all species, according to the literature [26–28], is a tbp (trigonal bipyramidal) arrangement.

The tartrate and malate systems are more difficult to study by means of this technique, as it is not possible to prepare more than one relevant point in the distribution diagram because precipitation occurs in the conditions of the measurements (i.e., $c_{Sn} = 10$ mmol dm^{-3}, $c_L = 40$ mmol dm^{-3}) at quite low pH, thus preventing an accurate proof or disproof of the models. As a consequence, the limited range of solution existence and the really noisy spectra make it impossible to test for a range of species, forcing us to estimate only the averaged effects of all the occurring structures. Experimental parameters for these species are

$$\text{Malate} : \delta = 3.5 \pm 0.8; \Delta = 1.3 \pm 0.1$$
$$\text{Tartrate} : \delta = 3.5 \pm 0.3; \Delta = 1.8 \pm 0.5$$

However, also for these ligands, the above reported parameters are compatible with the relative abundance of

Table 5 Observed Mössbauer parameters (mm s^{-1}) for Sn^{2+}/Cit system

	δ	Δ
Mononuclear	3.03 ± 0.03	2.12 ± 0.10
$Dinuclear_1$	3.12 ± 0.04	1.58 ± 0.10
$Dinuclear_2$	3.59 ± 0.09	1.83 ± 0.12

Data are reported as mean ± standard deviation

species obtained in the corresponding speciation diagrams, and with the tbp arrangement observed in the case of citrate.

Sequestering ability of various ligands

One of the most important applications of speciation studies is the evaluation of the sequestering ability of one or more different ligands toward one or more different metal ions in real systems, such as biological fluids, as well as natural and waste waters. This evaluation is frequently a challenging task, owing to the difficulties regarding, for example, the different number and/or nature of complexes formed. This last aspect is strictly correlated to the network of interactions occurring in a multicomponent system and, in particular, to the different complexing abilities of different ligand classes in different conditions and to the competition of the proton and/or hydroxide ion with metals and ligands involved in the sequestration process. To overcome the difficulty of simultaneously taking into account these factors, the use of a sigmoid Boltzmann-type equation was proposed [10–17]:

$$x = \frac{1}{1 + 10^{(\mathrm{pL} - \mathrm{pL}_{0.5})}} \quad (1)$$

where x is the fraction of the metal M (present in trace amounts) complexed by the ligand. The parameter $\mathrm{pL}_{0.5}$ (or pL_{50}), calculated by least-squares analysis, gives the analytical concentration of ligand necessary to sequester 50 % of the metal ($c_{\mathrm{L}} = 10^{-\mathrm{pL}0.5}$) and can be calculated once the conditions (pH, ionic strength, supporting electrolyte, temperature) are fixed and give an objective representation of the binding ability. Other details on the sequestering capacity expressed by Eq. (1) are reported in Refs. [10–17].

This function is a sigmoid curve (similar to a dose–response curve) with asymptotes of 1 for $\mathrm{pL} \to -\infty$ and 0 for $\mathrm{pL} \to +\infty$. It is important to note that this property varies with the experimental conditions, but it is independent of the analytical concentration of the metal ion when this is present as a trace amount in the system. However, one of the most important aspects to note is that in the calculation of $\mathrm{pL}_{0.5}$, all the side interactions occurring in the system (metal hydrolysis, ligand protonations, interactions with other components) are taken into account in the speciation model, but are excluded from the estimation of $\mathrm{pL}_{0.5}$ and do not make any contribution. In this way, the $\mathrm{pL}_{0.5}$ value is, in some ways, "cleaned" for all competing reactions.

In the case of the systems investigated here, the use of the $\mathrm{pL}_{0.5}$ is very useful, because it gives a clear picture not only of the sequestering ability of the ligands (Tar, Mala, and Cit) toward Sn^{2+}, but it also highlights the dependence of the sequestering ability of the ligands on the ionic strength (i.e., 0.15 and 1.00 mol dm^{-3}) and the ionic media (i.e., $NaCl_{(aq)}$ and $NaNO_{3(aq)}$) investigated. In particular, for the Sn^{2+}/Mala and Sn^{2+}/Cit systems, using the $\mathrm{pL}_{0.5}$ parameter, it is possible to calculate the different sequestering ability of the ligands toward Sn^{2+} in the two ionic media and to quantify the effect of the chloride anion on the sequestration of the metal.

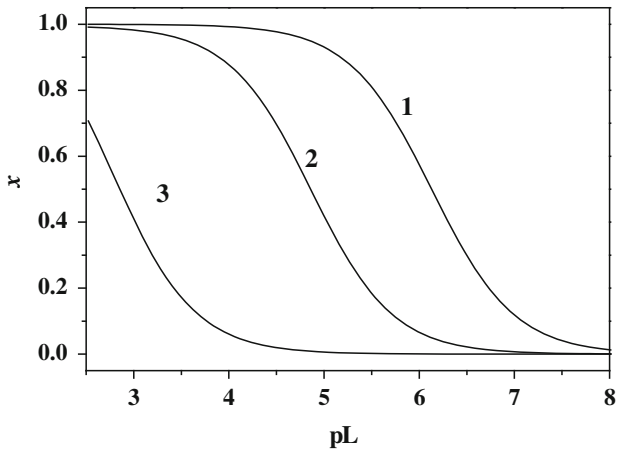

Fig. 6 Sequestration diagram for the Sn^{2+}/ligand systems in $NaCl_{(aq)}$ at $I = 0.15$ mol dm^{-3} and pH 5.0. Curves: *1* Tar ($\mathrm{pL}_{0.5} = 6.13$), *2* Cit ($\mathrm{pL}_{0.5} = 4.83$), *3* Mala ($\mathrm{pL}_{0.5} = 2.87$)

Figure 6 reports the $\mathrm{pL}_{0.5}$ values calculated for each system at $I = 0.15$ mol dm^{-3} in $NaCl_{(aq)}$.

At pH 5.0, the sequestering ability trend toward Sn^{2+} is

$$\text{Mala } (\mathrm{pL}_{0.5} = 2.87) < \text{Cit } (\mathrm{pL}_{0.5} = 4.83) < \text{Tar } (\mathrm{pL}_{0.5} = 6.13)$$

The $\mathrm{pL}_{0.5}$ values and the sequestering trend for Tar and Cit seem to be anomalous if we take into account the stability constants reported in Tables 2 and 4, where we can observe that the log K value of the ML species of the Sn^{2+}/Cit system is more than 2 log units higher than the value of the same species of the Sn^{2+}/Tar system. The higher sequestering ability of Tar can be interpreted by taking into account the protonation constants of the ligands: at pH 5.0, citrate is not completely deprotonated and is therefore less available to sequester the metal. This result is very useful to stress once again that, at least for complex systems, the sequestering ability of a ligand cannot be simply estimated by a superficial analysis of its stability constants, especially in environmentally or biologically relevant systems of high complexity. In contrast, because $\mathrm{pL}_{0.5}$ calculates the effective ligand concentration necessary to sequester the metals in the different experimental conditions, such as ionic strength, pH, temperature, it allows the direct comparison of the sequestering ability of one or more ligands in given conditions (the higher the $\mathrm{pL}_{0.5}$, the higher the sequestering ability is).

As stated before, changes in the ionic strength and in the ionic medium affect the speciation of the investigated Sn^{2+}/ligand systems: this would have an influence on the sequestering ability of these ligands toward tin(II), too. As an example, if we calculate the different sequestering ability of Mala toward Sn^{2+} in $NaCl_{(aq)}$ at $I = 0.15$ and 1.00 mol dm^{-3}, we observe that the $pL_{0.5}$ value at $I = 1.00$ mol dm^{-3} is higher than that at $I = 0.15$ mol dm^{-3} by $\sim$0.4 log units ($pL_{0.5} = 3.33$ and 2.87, respectively, at pH 5.0). The higher binding ability at $I = 1.00$ mol dm^{-3} can be explained by taking into account that the formation of the mixed $Sn_iH_jL_kCl_l^{(2i+j-kz-l)}$ species is of course favored at higher chloride concentrations than at $I = 0.15$ mol dm^{-3}. Moreover, the formation of the mixed species avoids the formation at low pH values of the $Sn(OH)_{2(s)}$ species, allowing Sn^{2+} to be more available for the interaction with the ligands. This is confirmed observing again the two distribution diagrams (Figs. 2, 3) of the conditional Sn^{2+}/Mala species drawn at $I = 1.00$ mol dm^{-3}; once more, in $NaCl_{(aq)}$ the formation of the $Sn(OH)_{2(s)}$ is significant only at pH >5, against a value of $\sim$4.4 in $NaNO_{3(aq)}$.

As a proof that different ligands show different behavior in different conditions, at pH 5.0 and $I = 1.00$ mol dm^{-3} in $NaNO_{3(aq)}$, we obtained quite different results in terms of sequestering ability ($pL_{0.5}$): 3.57 (Mala) < 5.02 (Tar) < 5.46 (Cit). In this case, citrate is able to interact more strongly with tin(II), because chloride is present in very low concentration (coming only from the dissolution of $SnCl_2$), and the $SnCl_l^{(2-l)}$ species are formed in negligible amounts.

$pL_{0.5}$ may also be used as an indirect check of the validity of the different approaches that can be used in the speciation studies. For example, we calculated the $pL_{0.5}$ of the Sn^{2+}/Mala system at $I = 1.00$ mol dm^{-3} in $NaCl_{(aq)}$ taking into account the two different approaches used for the speciation study, i.e., the model with the conditional stability constants (squares in Fig. 7), and the model that takes into account the mixed chloride species (circles in Fig. 7).

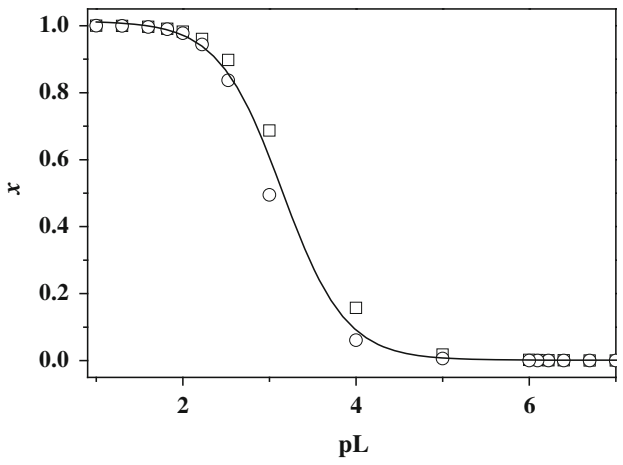

Fig. 7 Sequestration diagram of the Sn^{2+}/Mala system at $I = 1.00$ mol dm^{-3} and pH 5.0, using the different speciation approaches. *Squares* calculated from the conditional stability constants, *circles* calculated taking into account the stability constants in $NaNO_{3(aq)}$ and the mixed chloride species

Independently of the model used, it can be observed that the results are in good agreement; within the error of fits, a mean $pL_{0.5}$ value is obtained, i.e., $pL_{0.5} = 3.18 \pm 0.02$.

Temperature dependence and thermodynamic formation parameters

Potentiometric measurements carried out at different temperatures in $NaNO_{3(aq)}$ at $I = 1.00$ mol dm^{-3} allowed us to determine, for each simple $Sn_iH_jCit_k^{(2i+j-3k)}$ species, the corresponding formation enthalpy changes and entropies. The procedure adopted is detailed in the next section. The thermodynamic parameters of all these species are reported in Table 6.

The analysis of this table shows that the overall formation enthalpy changes of these species are all negative, indicating the exothermic nature of the overall complexation reaction of tin(II) by citrate. Table 6 also shows that the $T\Delta S$ values are generally positive and, mainly for the dimeric species, quite high. This evidences that, at least for these last species, their formation is an entropy-driven process. The tabulated ΔH values may be used in the Van't Hoff equation to calculate the stability constants of various $Sn_iH_jCit_k^{(2i+j-3k)}$ species at temperatures other than $T = 298.15$ K. However, for a faster calculation, the temperature dependence coefficients of each species are also reported for simplicity in the last column of Table 6. As expected from the negative enthalpy changes, all these

Table 6 Thermodynamic formation parameters of $Sn_iH_jCit_k^{(2i+j-3k)}$ species at $T = 298.15$ K and $I = 1.00$ mol dm^{-3} in $NaNO_{3(aq)}$

$i/j/k$[a]	ΔH[b]/ kJ mol^{-1}	ΔG/ kJ mol^{-1}	$T\Delta S$[b]/ kJ mol^{-1}	(Δlog $\beta/\Delta T$) × 1,000
1:1:0	−16.6	−41.9	25	−9.8
1:1:−1	−20.7	−17.1	−4	−12.2
1:1:−2	−28.6	31.7	−60	−16.8
2:2:2	−1.0	−138.2	137	−0.6
2:2:1	−3.9	−120.0	116	−2.3
2:2:0	−6.6	−103.3	97	−3.9
2:2:−1	−10.8	−77.9	67	−6.3
2:2:−2	−15.0	−52.2	37	−8.8

ΔH, ΔG, $T\Delta S$ values refer to Eq. (2)

[a] $i/j/k$ values refer to $Sn_iH_jCit_k^{(2i+j-3k)}$ species

[b] ±0.5–2.0 standard deviations

coefficients are negative, indicating that the stability of tin(II)/citrate complexes slightly decreases with increasing temperature.

Though the temperature dependence measurements have been performed for one system only, the considerations already made can be cautiously extended to the other hydroxocarboxylate/tin(II) systems, at least to have a rough idea of the complexation behavior of these ligands in the temperature conditions of some important real systems, for example, in the physiological conditions or at the temperatures of some natural waters.

TSTACO: another computer tool

Finally, it is important to mention here the procedure adopted for the data analysis of the measurements performed at different temperatures. The classical approach consists in determining the stability constants of various species at single temperature by the common calculation programs and only successively the log β values obtained at different temperatures are used to derive the corresponding formation enthalpy values by the Van't Hoff equation. In this work, this procedure has been automated by using a modified version of our calculation program STACO [29]. This version, called TSTACO, is briefly presented here for the first time, but before its presentation it has been tested in our laboratories for many years on different chemical systems, comparing the results of TSTACO with those obtained independently by the aforementioned classical procedure and/or by different experimental techniques (e.g., isoperibolic titration calorimetry). TSTACO is based on the simultaneous elaboration of data derived from a wide number of potentiometric titrations performed at the same ionic strength but at different temperatures. By non-linear least-squares calculations using the algorithm derived from STACO, it is possible to refine both the stability constants and the corresponding formation enthalpy changes simultaneously. In developing the program, the possibility of refining the ΔC_p values has also been taken into account for measurements performed in wide temperature ranges, where this term cannot be neglected (i.e., the temperature dependence of ΔH must be considered), according to the Clarke and Glew equation [30].

Concerning the input file, the only difference between the original STACO and TSTACO is that, in the latter, (i) the temperature values must be specified for each single measurements and (ii) in addition to the stability constants of other species than those to be refined, the corresponding formation enthalpy changes must be added. In the case of the Sn^{2+}/citrate system, the ΔH values for pK_w, tin(II) hydrolysis and the citrate protonation were necessary and were taken from Refs. [1] and [31].

Experimental

Chemicals

L(+)-Tartaric (Tar), L(−)-malic (Mala), and citric acid (Cit) solutions were prepared by weighing the pure acids. The ligand purity, checked by alkalimetric titrations, was always at least 99.5 %. Tin(II) chloride solutions were prepared by weighing the dihydrated pure salt. The concentration was checked against EDTA standard solutions and the purity was always at least 99 %. Particular attention was paid to the preparation of these solutions, in order to prevent oxidation of Sn^{2+} to Sn^{4+} and to hamper the formation of soluble and sparingly soluble hydrolytic species. The solutions were acidified with HCl to pH <2 and a piece of metallic tin was added to the solutions after the preparation. The solutions were immediately bubbled with purified N_2 to exclude any O_2 traces and used always immediately after the preparation. Nitric acid, hydrochloric acid, and sodium hydroxide solutions were prepared by diluting concentrated ampoules and were standardized against sodium carbonate and potassium hydrogen phthalate, respectively. $NaNO_3$ and NaCl solutions were prepared by weighing the pure salts dried in an oven at $T = 383.15$ K. All solutions were prepared with analytical grade water ($R = 18$ MΩ cm^{-1}) using grade A glassware. All the chemicals had the highest available purity and were purchased from Sigma-Aldrich (Italy).

Apparatus and procedure for potentiometric measurements

Potentiometric measurements were carried out (at $T = 298.15 \pm 0.10$ K in thermostatted cells) by two operators using two different setups, in order to minimize systematic errors and to check the repeatability of the measurements. The first setup consisted of a 713 Metrohm potentiometer equipped with a half-cell glass electrode (Ross type 8101, from Thermo-Orion) and a double-junction reference electrode (type 900200, from Thermo-Orion), and a 765 Metrohm motorized burette. The apparatus was connected to a PC and automatic titrations were performed using a suitable homemade computer program to control titrant delivery, data acquisition, and to check for e.m.f. stability. The second setup consisted of a 809 Metrohm Titrando apparatus controlled by Metrohm TiAMO 1.2 software equipped with a combination glass electrode (Ross type 8102, from Thermo-Orion). Estimated precision was ±0.15 mV and ±0.003 cm^3 for the e.m.f. and titrant volume readings, respectively, and was the same for both setups. All the potentiometric titrations were carried out under magnetic stirring and bubbling purified presaturated N_2 through the solution, in order to exclude O_2 and CO_2.

Titrand solutions were prepared by addition of different amounts of the ligands ($1.0 \leq c_L$/mmol dm$^{-3} \leq 5.0$), tin(II) ($0.5 \leq c_{Sn}$/mmol dm$^{-3} \leq 2.1$), and the supporting electrolyte (NaCl or $NaNO_3$) to obtain the pre-established ionic strength values (0.15 and 1.00 mol dm^{-3} in $NaCl_{(aq)}$, and 1.00 mol dm^{-3} in $NaNO_{3(aq)}$). Since the ligands were used in their acidic form and known amounts of acid were already present in tin(II) solutions, further acid additions were unnecessary. Potentiometric measurements were carried out by titrating 25 or 50 cm^3 of the titrand solutions with standard NaOH solutions up to the pH where the formation of scarcely soluble species was noted. For each experiment, independent titrations of strong acid solutions with standard base were carried out under the same medium and ionic strength conditions as the systems to be investigated, with the aim of determining the electrode potential (E^0) and the acidic junction potential ($E_j = j_a$ [H$^+$]). In this way, the pH scale used was the free scale, pH $= -\log_{10}$[H$^+$], where [H$^+$] is the free proton concentration (not activity). The reliability of the calibration in the alkaline pH range was checked by calculating the appropriate pK_w values. For each titration, 80–100 data points were collected and the equilibrium state during titrations was checked by adopting some usual precautions [32]. These included checking the time required to reach equilibrium and performing back titrations.

For the temperature dependence measurements for the Sn^{2+}/Cit system at $I = 1.00$ mol dm^{-3} in $NaNO_{3(aq)}$, the same titrations performed at $T = 298.15 \pm 0.10$ K were also repeated at $T = 283.15$ and 310.15 ± 0.10 K.

Apparatus and procedure for Mössbauer measurements

All samples were freshly prepared at the required concentration and then adjusted to the desired pH. Aqueous tin(II)/ligand solutions ($c_{Sn} = 10$ mmol dm^{-3}, $c_L = 40$ mmol dm^{-3}, $I = 0.15$ mol dm^{-3} in $NaNO_{3(aq)}$) were then transferred in PET sample holders (ø 14 mm, sample thickness 10 mm) and quickly frozen in liquid N_2. Spectra were collected to $\sim 5 \times 10^5$ counts per channel at a resolution of 512 channels. The Mössbauer spectra were recorded with a conventional spectrometer operating in transmission mode, using a 10 mCi $Ca^{119}SnO_3$ source (Ritverc GmbH, St. Petersburg, Russia) moving at room temperature with constant acceleration in a triangular waveform. The driving system, multichannel analyzer, proportional counter detector, and related electronics were purchased from TAKES (Ponteranica, Italy). The samples were kept at liquid nitrogen temperature by means of an NRD-1258-DMB (Cryo Industries, USA) cryostat. Channel calibration was performed using a 10 mCi ^{57}Co/Rh source on a 4-μm-thick α^{57}Fe foil absorber (both Ritverc GmbH). Reported isomer shifts (δ) are relative to room temperature $Ca^{119}SnO_3$.

Calculations

The non-linear least-squares computer program ESAB2M was used to refine all the parameters of the acid–base titration (E^0, K_w, liquid junction potential coefficient j_a, analytical concentration of reagents). The BSTAC and STACO computer programs were used to calculate the complex formation constants. Both programs can deal with measurements at different ionic strengths. The ES4ECI program was used to draw speciation and sequestration diagrams and to calculate species formation percentages. More details on the computer programs are given in Ref. [18]. The TSTACO program used for the temperature dependence calculations is briefly described in the dedicated section.

Hydrolysis, protonation, and complex formation constants are given according to the following equilibrium:

$$i\ Sn^{2+} + j\ H^+ + k\ L^{z-} + l\ Cl^- = Sn_iH_jL_kCl_l^{(2i+j-kz-l)}\ \beta_{ijkl} \quad (2)$$

When $i = l = 0$, Eq. (2) refers to the ligand protonation constants, whereas when $k = l = 0$ and $j < 0$, Eq. (2) refers to the metal hydrolysis constants. Formation constants, concentrations, and ionic strengths are expressed in the molar concentration scale (c, mol dm^{-3}), and errors are expressed as ±standard deviation. The charges of the various species are sometimes omitted for simplicity.

Acknowledgments The authors thank the Universities of Messina and Palermo for partial financial support.

References

1. Cigala RM, Crea F, De Stefano C, Lando G, Milea D, Sammartano S (2012) Geochim Cosmochim Acta 87:1
2. Cigala RM, Crea F, De Stefano C, Lando G, Manfredi G, Sammartano S (2012) J Mol Liquids 165:143
3. Cigala RM, Crea F, De Stefano C, Lando G, Milea D, Sammartano S (2012) J Chem Thermodyn 51:88
4. Bulten EJ, Meinema HA (1991) Tin. In: Merian E (ed) Metals and their compounds in the environment. Occurrence, analysis and biological relevance. VCH, Weinheim, p 1243
5. Anger JP (2004) Tin. In: Merian E, Anke M, Ihnat M, Stoeppler M (eds) Elements and their compounds in the environment, 2nd edn. Wiley-VCH Verlag, Weinheim, p 1113
6. Rosenberg E (2005) Speciation of tin. In: Cornelis R, Crews H, Caruso J, Heumann KG (eds) Handbook of elemental speciation II: species in the environment, food, medicine and occupational health. Wiley, Chichester, p 422
7. Séby F, Potin-Gautier M, Giffaut E, Donard OFX (2001) Geochim Cosmochim Acta 65:3041
8. Nelson DL, Cox MM (2008) Lehninger principles of biochemistry, 5th edn. Freeman, New York
9. Berto S, Crea F, Daniele PG, Gianguzza A, Pettignano A, Sammartano S (2012) Coord Chem Rev 256:63
10. Casale A, De Stefano C, Manfredi G, Milea D, Sammartano S (2009) Bioinorg Chem Appl 2009:219818. doi:10.1155/2009/219818

11. Crea F, De Stefano C, Milea D, Sammartano S (2009) J Solution Chem 38:115
12. Crea F, De Stefano C, Milea D, Sammartano S (2010) Monatsh Chem 141:511
13. De Stefano C, Lando G, Milea D, Pettignano A, Sammartano S (2010) J Solution Chem 39:179
14. Gianguzza A, Milea D, Pettignano A, Sammartano S (2010) Environ Chem 7:259
15. Berto S, Crea F, Daniele PG, De Stefano C, Prenesti E, Sammartano S (2012) Radiochim Acta 100:13
16. Gianguzza A, Giuffrè O, Piazzese D, Sammartano S (2012) Coord Chem Rev 256:222
17. Bretti C, Cigala RM, Lando G, Milea D, Sammartano S (2012) J Agric Food Chem 60:8075
18. De Stefano C, Sammartano S, Mineo P, Rigano C (1997) Computer tools for the speciation of natural fluids. In: Gianguzza A, Pelizzetti E, Sammartano S (eds) Marine chemistry: an environmental analytical chemistry approach. Kluwer, Amsterdam, p 71
19. Foti C, Sammartano S (2010) J Chem Eng Data 55:904
20. Crea F, Milea D, Sammartano S (2005) Talanta 65:229
21. Crea F, Milea D, Sammartano S (2005) Ann Chim (Rome) 95:767
22. Crea P, De Stefano C, Milea D, Sammartano S (2008) Mar Chem 112:142
23. Amico P, Daniele PG, Ostacoli G, Arena G, Rizzarelli E, Sammartano S (1985) Transition Met Chem 10:11
24. Daniele PG, De Robertis A, Ostacoli G, Sammartano S, Zerbinati O (1988) Transition Met Chem 13:87
25. Daniele PG, De Robertis A, De Stefano C, Gianguzza A, Sammartano S (1990) J Chem Res (S) 300: (M) 2316
26. Arifin Z, Filmore EJ, Donaldson JD, Grimes SM (1984) J Chem Soc Dalton Trans 1965
27. Cheng HS, Hsu CM, Shih LL (1984) J Chin Chem Soc 31:117
28. Donaldson JD, Grimes SM, Nicolaides A, Smith PJ (1985) Polyhedron 4:391
29. De Stefano C, Foti C, Giuffrè O, Mineo P, Rigano C, Sammartano S (1996) Ann Chim (Rome) 86:257
30. Clarke ECW, Glew DN (1966) Trans Faraday Soc 62:539
31. De Stefano C, Foti C, Giuffrè O, Sammartano S (2001) J Chem Eng Data 46:1417
32. Braibanti A, Ostacoli G, Paoletti P, Pettit LD, Sammartano S (1987) Pure Appl Chem 59:1721